MULTI-RESPONSE OPTIMIZATION OF GEOPOLYMER MORTAR AT ELEVATED TEMPERATURES

MARIAM FAROUK GHAZY [1*] , METWALLY ABD ALLAH ABD ELATY[1], MOHAMED FATTOUH ABD EL HAMEED[2]

[1]*Faculty of Engineering, Structural Engineering department, Tanta University, Tanta, Egypt*
[2]*Faculty of Engineering, Department of Production Engineering and Mechanical Design, Minufiya University, Egypt*

In this study a hybrid method including a response surface methodology, technique for order preference by similarity to ideal solution (TOPSIS), and a particle swarm optimization (PSO) algorithm were proposed to determine optimal parameter settings of the geopolymer (GP) mortar. Compressive strength, flexural strength, splitting tensile strength, and weight loss were used as the most important characteristics. Six factors (metakaolin, cement, sodium silicate solution, polypropylene fibers, curing temperature, and elevated temperature) each at three levels with 54 experiments was selected. TOPSIS method was used to convert the single-responses to an equivalent single-response known as a multi-performance characteristics index (MPCI). The significance of the process parameters was also evaluated using the analysis of variance. The PSO was used to predict optimal parameter settings of the GP-mortar process. The approach and the methodologies employed in this work can be utilized in solving the mixture proportions of the optimization problem.

Keywords: *Geopolymer motar; Response surface methodology; TOPSIS; Particle swarm optimization; Mechanical properties; elevated temperature*

1. Introduction

The geopolymer (GP) is a promising candidate as an alternative to ordinary Portland cement for developing various sustainable products in making building materials, concrete, fire resistant coatings, fiber reinforced composites and waste immobilization solutions for the chemical and nuclear industries. Research findings revealed that GP concrete exhibited comparative properties to that of OPC concrete which has potential to be used in civil engineering applications [1].

GP are generally believed to provide good fire resistance due to their ceramic-like properties [2,3]. The effect of elevated temperature on GP paste, mortar and concrete made using fly ash (FA) as a precursor was studied. Various experimental parameters have been examined such as specimen sizing, aggregate sizing, aggregate type and superplasticizer type [2]. Meanwhile, the effects of molarities, curing regimes and aggregate size on the strength properties of GP concretes at elevated temperatures were also reported [3]. The strength of the GP paste, mortar and concrete before exposure were approximately the same. However, the strength losses after elevated temperature exposure at 600 °C were 73.4, 100 and 58.4%, for paste, mortar and concrete, respectively [2].

The effect of elevated temperatures on GP mortar and concrete for different types of coarse and fine aggregates were conducted and compared with the OPC concrete of grade M20 for temperature exposures up to 500 °C. The results showed that the compressive strength of the GP mortars increase up to 100 ºC and after that it starts to decrease. After exposure to 500 ºC, the decrease in strength of GP mortar is 69.76% while OPC mortar has zero strength [4]. Some initial studies showed that FA based GPs gained strength at exposure to relatively low temperature heat such as 200 °C and lost strength at exposure to heats of higher temperature [5,6].

The strength loss in the GP concrete specimens was mainly because of the difference between the thermal expansions of GP matrix and the aggregates [2,7].

GP binders made with 50% MK and 50% FA provide optimum bending and compressive strengths both at ambient temperature and after exposure to high temperatures (800 °C) [8].

Fiber reinforcement is often used to improve the mechanical properties [9] and the resistance of materials to dehydration damage during high temperature exposure [10-12]. However, a GP made with 50% MK and 50% FA and reinforced by 2% carbon fibers can be an effective alternative material for structures in fire resistance applications [12].

Development of GP concrete became a necessity to widen its applications beyond precast concrete. The inclusion of 5% OPC in low calcium FA reduced the setting time to acceptable ranges and caused slight decrease of workability. The early-age compressive strength improved significantly with higher strength at the age of 28 days. GP microstructure showed considerable portion of calcium-rich aluminosilicate gel resulting from the addition of OPC [13]. The use of 10% OPC in GP

*Autor corespondent/*Corresponding author*,
E-mail: mariam.ghazy@f-eng.tanta.edu.eg ; dr.mariamghazi@yahoo.com

mortar improved the modulus of rupture and fracture characteristics [14].

Limited researches were conducted on inclusion of OPC-PP fiber reinforced GP composites at elevated temperature.

Because the GP mortar consists of many conflicting factors; it is critical to use a systematic methodology to determine the optimal mixes and to analyze the most effective factors under a set of constraints. Recovering only one feature of GP mortar without considering other features restricts industrial applications of the product. All criteria require to be simultaneously optimized if products are to find application area in industry. In order to get desired quality, finding optimal mix ratio of GP mortar is quite important issue on material and design engineering. Many optimization and modeling methods based on experimental design have been suggested. Response Surface Methodology (RSM) has been used [15,16]. Taguchi method has also been used [17,18]. The TOPSIS method is quite simple and adaptable compared to other multi attribute decision making, such as principal component analysis (PCA) [19], and Grey relational analysis (GRA) [20]. Recently, the TOPSIS based Taguchi method has been utilized to solve the multi-response optimization problems [21]. However, TOPSIS based Taguchi method can only find the best specified process parameter level combination which includes the discrete setting values of process parameters, and it cannot help engineers obtain optimal process parameter when the process parameter variables are continuous. Therefore, a clear mathematical model and a systematical optimization method that can be generally used in process optimization are still required.

The authors are not aware of any literature that discusses the multi-response optimization problem by using TOPSIS-based RSM. For this reason, this research proposes a hybrid, TOPSIS-based RSM and PSO algorithm to optimize and investigate the ranking of the conflicting factor levels and the best possible mix proportions of the GP mortar. First of all, factors and their levels effect on the performance characteristics of GP mortar have been defined. Then, the experiments have been carried out according to runs determined by RSM and the results (decision matrix) was obtained. The TOPSIS method was used to transform the multi-response problem into a single-response problem and can provide a ranking index to represent the multi performance characteristics index (MPCI) of GP mortar. The relation among factors and the MPCI of GP mortar was determined by the RSM using Design Expert statistical program package.

2. Research significance

The main objective of this study lies in the use of TOPSIS based on design of experiment coupled with PSO algorithm to assess the effects of mixture components on the MPCI of the GP mortar at elevated temperatures. It will be helpful to the engineers in deciding the near optimal combination parameters of GP mortar for desired MPCI especially at elevated temperatures.

3. Experimental work

3.1 Materials

Commercially available materials were used in this investigation. Class F fly ash (FA) as classified by ASTM C618-20 [22] was used as based material for GP mortar mixes. Metakaolin (MK) was produced by the thermal treatment of kaolinite at 800 °C in an automatic electric furnace for 2 h. The specific gravity of the used MK was 2.7, and the Blaine specific surface area was ≈35 m^2/g. MK was used as partial replacement by weight of FA with 10%, 20%, and 30%. Portland cement (C) CEM I 42.5N type conforming to EN 197-1 [23] with Grade 42.5N was used. Cement (C) was used with 5%, 10%, and 15% as partial replacement by weight of FA. Natural siliceous sand was used as fine aggregates conforming to the ASTM C33 [24] with 100% passing through sieve size 4.75 mm, and a specific gravity of 2.6. A combination of sodium hydroxide (NH) and sodium silicate solution (NS) with 0.4 of total binder was used as alkaline activator solutions (AS). NH in flake form with a 98% purity and the NS solution (Na_2O = 14.7%, SiO_2 = 29.4% and water = 55.9% by mass) were used. Three different ratios of NS (0.65, 0.7 and 0.75) were used. Tap water (W), was used for extra water with 10% weight of the total binder (FA+MK+C) and to preparing the NH solution with 12M and 1.4 specific gravity. The AS was prepared one day prior to its use. Polypropylene fiber (PP), (FIBERMESH) with 19 mm in length and 0.04 mm equivalent diameter was used at three different contents of 0, 0.5, and 1% (by volume of GP). The average tensile strength, elastic modulus of the PP, and the ultimate elongation were 600 MPa and 6 GPa, and 8%, respectively.

3.2 Specimens preparation, curing and test methods

Fifty-four mixes were prepared and poured to carry out the experimental program as given in Table 1. The ratio of binder content (FA+MK+C) to fine aggregate (sand) is 1:1.5. Mixing procedures were carried out in a rotary mixer of 5 L total capacity. The FA was first mixed for 2 min with the AS after that MK was added and mixed for 1 min. Extra water was then added and mixed for 1 min. The mixture was allowed to rest for 30 s and the walls were scraped and then mixed continuously for 1 min. Then, sand was continuously added and mixed for 3 min. Cement was added and mixed for another 1 min. Finally, PP fibers (if applicable) were then slowly added to the mix and the mixing continued until the fibers were well dispersed

Table 1

Experimental plan and test results

Mix No.	Control variables						Test results				
	MK	C	NS	F	CT, ºC	ET, ºC	Flow, mm	Fc, MPa	Fr, MPa	Ft, MPa	WL%
1	0.1	0.05	0.7	0	50	412	225	18.67	3.38	1.71	1.06
2	0.3	0.05	0.7	0	50	412	205	20.91	2.16	2.16	0.99
3	0.1	0.15	0.7	0	50	412	210	11.06	3.00	1.20	1.19
4	0.3	0.15	0.7	0	50	412	175	17.20	3.40	1.70	1.48
5	0.1	0.05	0.7	0.01	50	412	175	14.34	4.67	1.65	0.52
6	0.3	0.05	0.7	0.01	50	412	180	20.61	4.00	2.23	0.67
7	0.1	0.15	0.7	0.01	50	412	175	10.58	2.50	1.11	0.50
8	0.3	0.15	0.7	0.01	50	412	155	16.20	3.18	1.76	0.83
9	0.2	0.05	0.65	0.005	25	412	180	30.50	3.86	2.09	1.99
10	0.2	0.15	0.65	0.005	25	412	185	13.10	2.51	1.11	2.29
11	0.2	0.05	0.75	0.005	25	412	195	32.75	4.15	1.60	1.22
12	0.2	0.15	0.75	0.005	25	412	145	25.16	3.75	0.78	0.90
13	0.2	0.05	0.65	0.005	75	412	180	31.92	5.08	2.05	1.17
14	0.2	0.15	0.65	0.005	75	412	180	23.93	4.00	1.90	1.55
15	0.2	0.05	0.75	0.005	75	412	175	25.50	4.10	1.79	2.67
16	0.2	0.15	0.75	0.005	75	412	120	21.90	3.28	1.50	2.83
17	0.2	0.1	0.65	0	50	25	220	24.20	6.50	3.83	0
18	0.2	0.1	0.75	0	50	25	220	20.54	5.40	3.21	0
19	0.2	0.1	0.65	0.01	50	25	170	26.49	6.38	3.40	0
20	0.2	0.1	0.75	0.01	50	25	165	26.79	5.74	3.18	0
21	0.2	0.1	0.65	0	50	800	220	18.20	1.50	1.36	2.60
22	0.2	0.1	0.75	0	50	800	220	14.20	0.92	0.98	2.57
23	0.2	0.1	0.65	0.01	50	800	170	9.25	1.03	1.29	3.00
24	0.2	0.1	0.75	0.01	50	800	165	11.97	0.86	0.92	2.95
25	0.1	0.1	0.7	0	25	412	230	16.39	3.03	1.01	1.97
26	0.3	0.1	0.7	0	25	412	195	30.20	3.09	1.72	2.00
27	0.1	0.1	0.7	0.01	25	412	205	14.46	3.50	0.87	1.78
28	0.3	0.1	0.7	0.01	25	412	165	25.13	3.66	1.36	2.03
29	0.1	0.1	0.7	0	75	412	240	27.01	4.70	1.53	2.62
30	0.3	0.1	0.7	0	75	412	205	26.11	3.84	2.06	2.58
31	0.1	0.1	0.7	0.01	75	412	170	22.41	4.00	1.65	2.06
32	0.3	0.1	0.7	0.01	75	412	160	23.61	3.55	1.88	2.70
33	0.2	0.05	0.7	0.005	25	25	160	38.25	6.46	3.77	0
34	0.2	0.15	0.7	0.005	25	25	175	23.69	6.07	2.70	0
35	0.2	0.05	0.7	0.005	75	25	160	49.97	8.00	5.00	0
36	0.2	0.15	0.7	0.005	75	25	130	41.40	7.80	4.30	0
37	0.2	0.05	0.7	0.005	25	800	160	31.80	1.58	2.00	2.90
38	0.2	0.15	0.7	0.005	25	800	175	26.00	1.75	1.50	2.90
39	0.2	0.05	0.7	0.005	75	800	160	14.52	1.24	1.20	3.85
40	0.2	0.15	0.7	0.005	75	800	130	15.63	1.43	1.66	4.23
41	0.1	0.1	0.65	0.005	50	25	205	27.00	6.28	2.60	0
42	0.3	0.1	0.65	0.005	50	25	190	28.01	6.24	4.59	0
43	0.1	0.1	0.75	0.005	50	25	195	21.14	6.04	2.35	0
44	0.3	0.1	0.75	0.005	50	25	170	27.24	5.50	4.20	0
45	0.1	0.1	0.65	0.005	50	800	205	15.61	0.95	1.57	2.79
46	0.3	0.1	0.65	0.005	50	800	190	15.59	0.93	1.00	2.80
47	0.1	0.1	0.75	0.005	50	800	195	14.00	1.52	1.42	2.39
48	0.3	0.1	0.75	0.005	50	800	170	13.90	0.98	0.70	2.68
49	0.2	0.1	0.7	0.005	50	412	195	30.44	3.53	1.90	1.67
50	0.2	0.1	0.7	0.005	50	412	190	30.34	3.50	2.00	1.70
51	0.2	0.1	0.7	0.005	50	412	193	30.45	3.53	2.05	1.65
52	0.2	0.1	0.7	0.005	50	412	195	30.40	3.48	1.90	1.67
53	0.2	0.1	0.7	0.005	50	412	193	30.34	3.50	1.90	1.70
54	0.2	0.1	0.7	0.005	50	412	194	30.44	3.53	2.00	1.67

Where: C: cement, MK: metakaolin, NS: sodium silicate solution, F: polypropylene fibers, CT: curing temperatures, ET: elevated temperatures, Fc: compressive strength, Fr: flexural strength, Ft: splitting tensile strength, WL: weight loss (at least for 2 min). After mixing process, the mortar samples were tested for flowability in accordance with ASTM C1437 [25]. It can be seen that the consistency reduced noticeably with increasing of C. Moreover, increasing MK and the fiber volume fraction resulted in a reduction in the flow. Meanwhile, the increase of NS slightly reduced the consistency of the investigated mixes.

The GP mortar mixes were cast into the molds and compacted in two layers using a vibrating table for 30 s to release any residual air bubbles. Specimens were stored in ambient temperature at 25 °C and 50% RH leaving the top surface exposed to air. After 24 h of casting, specimens were demolded and then cured by certain curing temperature (CT) (25 °C, 50 °C and 75 °C) (curing in ambient temperature at (25 °C and 50% RH), or heat curing in an isothermal environmental chambers at a temperatures of 50 or 75 °C for 48 h) and at the end of curing the specimens were kept in ambient temperature at (25 °C and 50% RH) until the day of testing after 28 days. Prismatic specimens of size 40x40x160 mm were poured and used for obtaining flexural strength (Fr) and compressive strength (Fc) in accordance with EN 196-1 [26]. The splitting tensile strength (Ft) was evaluated using cylindrical specimens of 50x100 mm according to Brazilian Standard NBR 7222 [27]. Three elevated temperatures (ET) (25 °C, 412 °C and 800 °C) were used (for specimens exposed to 25 °C, the specimens were lift in ambient temperature at (25 °C and 50% RH) as a control one. For specimens exposed to ET (412, 800 °C), the hardened GP mortar specimens were first dried for 24 h in an electric oven at a temperature of 105 °C to remove the free water. Then, they were kept for 2 h at required exposed temperatures in electric furnace (once the required temperature was attained, it was maintained for further 2 h). The specimens were allowed to cool gradually by left in the laboratory temperature. Hydraulic Compression-Flexure Testing Machine of total capacity 300 kN was used for testing specimens. Moreover, the weight loss (WL) after exposure to ET were calculated for each specimen.

3.3 Methods of analysis used in the study

In this section, the brief summaries of each of the methods, namely RSM, preference by similarity to ideal solution (TOPSIS) method, and particle swarm optimization (PSO) algorithm, are given.

3.3.1 Response Surface Methodology (RSM)

RSM is a well-known design of experiment (DOE) methodology and it has been widely employed in various manufacturing process optimization studies [28,29]. RSM is a collection of mathematical and statistical technique useful for analyzing problems in which several independent variables influence a dependent variable or response and the goal is to optimize the response [30]. In many experimental conditions, it is possible to represent independent factors in quantitative form as given in the second-order regression model Eq. (1):

$$
\begin{aligned}
y = \beta_0 &+ \beta_1 x_1 + \beta_2 x_2 + \ldots \\
&+ \beta_k x_k + \beta_{11} x_1^2 + \beta_{22} x_2^2 + \ldots \\
&+ \beta_{kk} x_k^2 + \beta_{12} x_1 x_2 + \ldots + \beta_{k-1,k} x_{k-1} x_k
\end{aligned}
\tag{1}
$$

Where, $(\beta_1, \beta_2 \ldots \beta_k)$ coefficients for main effects, $(\beta_{11}, \beta_{22} \ldots \beta_{kk})$ coefficients for quadratic main effects and $(\beta_{12}, \beta_{13} \ldots \beta_{k-1,k})$ coefficients for two factor interaction effects. In order to estimate the regression coefficients, a number of experimental design techniques are available. In this work, Box-Behnken design matrix was used which accurately fits the second order response surfaces. This matrix requires three levels of each factor. All the coefficients of the second order were obtained using the Design Expert statistical software package. The adequacy of the developed model can be tested using the analysis of variance (ANOVA). After determining the significant coefficients (at 95% confidence level), the final model was developed using only these coefficients.

3.3.2 Preference by similarity to ideal solution (TOPSIS) method

TOPSIS method was firstly proposed by (Hwang and Yoon, 1981) [31]. The basic concept of this method is that the chosen alternative (appropriate alternative) should have the shortest distance from the positive ideal solution and the farthest distance from negative ideal solution. Positive ideal solution is a solution that maximizes the benefit criteria and minimizes adverse criteria, whereas the negative ideal solution minimizes the benefit criteria and maximizes the adverse criteria. The TOPSIS process is used to combine all identified performance values of the system into a single value that can then be used as a single performance in the multi-response optimization issues. The steps involved in TOPSIS method are as follows [32]:

Step 1: This step involves the development of matrix format. The row of this matrix is allocated to one alternative and each column to one attribute. The decision-making matrix can be expressed as Eq. (2):

$$
D = \begin{array}{c} A_1 \\ A_2 \\ \cdot \\ A_j \\ \cdot \\ A_m \end{array}
\begin{bmatrix}
x_{11} & x_{12} & \cdot & x_{1l} & x_{1n} \\
x_{21} & x_{22} & \cdot & x_{2j} & x_{2n} \\
\cdot & \cdot & \cdot & \cdot & \cdot \\
x_{i1} & x_{i2} & \cdot & x_{ij} & \cdot \\
\cdot & \cdot & \cdot & \cdot & \cdot \\
x_{m1} & x_{m2} & \cdot & x_{mj} & x_{mn}
\end{bmatrix}
\tag{2}
$$

Where, A_i (i = 1,2,…,m) represents the attributes (responses) related the possible alternative (experimental number); x_j (j = 1,2,…,n)

represents the attributes related to alternative performance, j = 1,2,…,n and x_{ij} is the performance of A_i with respect to attribute x_j.
Step 2: Obtain the normalized decision matrix r_{ij}. This can be represented as Eq. (3):

$$r_{ij} = \frac{x_{ij}}{\sqrt{\sum_{i=1}^{m} x_{ij}^2}} \quad (3)$$

Where, r_{ij} represents the normalized performance of A_i with respect to attribute x_j, i = 1,…,m and j=1,…,n.
Step 3: Obtain the weighted normalized decision matrix V=[v_{ij}] and can be found as Eq. (4):

$$V = w_j \, r_{ij} \quad (4)$$

Where, $\sum_{j=1}^{n} w_j = 1$

Step 4: Identification of positive ideal and negative ideal solutions (A^+ and A^-):

The positive ideal solution, A^+ (A_i^+; i = 1,2,…,m), is made of all the best values and the negative-ideal solution, A^- (A_i^-; i = 1,2,…,m), is made of all the worst values at the responses in the weighted normalized decision matrix (V). They are calculated by using Eqs. (5 and 6).

The ideal solution:

$$A^+ = \{(\max_i v_{ij} \,|\, j \in J), (\min_i v_{ij} \,|\, j \in J' \,|\, i = 1,2,....,m)\} = \{v_1^+, v_2^+, ..., v_j^+, ..., v_n^+\} \quad (5)$$

The negative ideal solution:

$$A^- = \{(\min_i v_{ij} \,|\, j \in J), (\max_i v_{ij} \,|\, j \in J' \,|\, i = 1,2,....,m)\} = \{v_1^-, v_2^-, ..., v_j^-, ..., v_n^-\} \quad (6)$$

Where, $J = \{j = 1,2,....,n \,|\, j\}$: Associated with the beneficial attributes and $J' = \{j = 1,2,....,n \,|\, j\}$: Associated with non-beneficial adverse attributes

Stop 5: Calculation of the separation measures: the distance of an alternative (experimental number) i to the positive ideal solution (S_i^+), and the distance from the negative ideal solution (S_i^-) are calculated by using Eqs. (7 and 8).

$$S_i^+ = \sqrt{\sum_{j=1}^{n} (v_{ij} - v_j^+)^2}, i = 1,2,....,m \quad (7)$$

$$S_i^- = \sqrt{\sum_{j=1}^{n} (v_{ij} - v_j^-)^2}, i = 1,2,....,m \quad (8)$$

Step 6: Calculate the relative closeness to the ideal solution Eq. (9):

$$C_i^+ = \frac{S_i^-}{S_i^+ + S_i^-}, \; i = 1,2,...., \; m; 0 \le C_i^+ \le 1 \quad (9)$$

Step 7: Rank the preference order. The alternative with the largest relative closeness is the best choice. In the present study C_i^+ for each product has been termed as MPCI.

3.3.3 Particle swarm optimization (PSO) algorithm

The PSO algorithm, first proposed by Kennedy and Eberhart (1995) [33]. Like other evolutionary algorithms, PSO is also a population-based optimization algorithm. PSO is rooted upon imitating the choreography of bird flocks that communicate together as they fly; therefore, the population is called “swarm”, while, the potential solutions are named as “particles”. Particles iteratively fly over the search space in explicit directions and are attracted to self attained historical best position (personal best; pbest), as well as the best position among the entire swarm (global best; gbest). Each particle records the coordinates of the best location it has visited so far. For simplicity and avoiding lengthy statement the concept and mathematical steps of PSO algorithm were presented and employed in references [34]. A detailed flowchart of PSO is shown in Fig. 1.

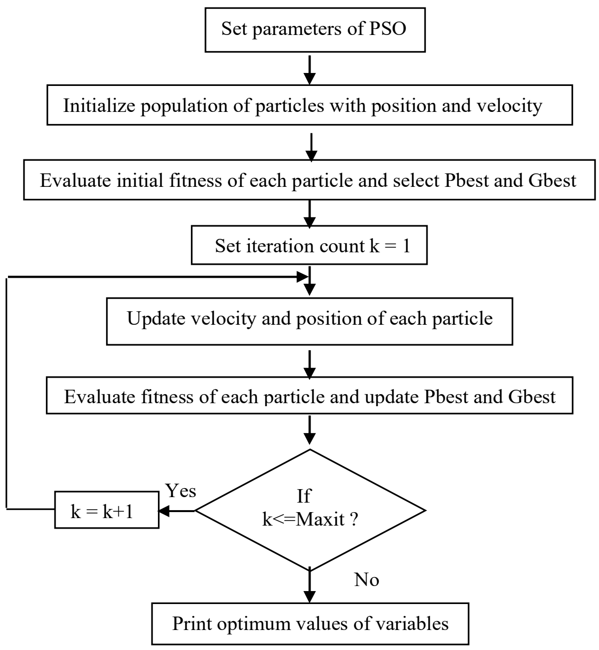

Fig. 1 - Flowchart of PSO.

4. Results and discussions

An experimental study to determine optimal parameter settings of the GP mortar was conducted and the test results are presented in Table 1. The mechanical properties and the weight loss were evaluated. In fact, realizing the influence of each parameter solely on the target responses cannot be completely achieved by direct analysis methods due to the interactions between them. So, the following sections present in detail statistical analysis for the influence of each parameter.

Table 2

Evaluated relative closeness (C^+=MPCI)

Mix No.	Weight normalized value (V_{ij})				Separation measures		Relative closeness
	Fc	Fr	Ft	WL	S^+	S^-	C^+=MPCI
1	0.041	0.034	0.021	0.007	0.092	0.041	0.308
2	0.046	0.021	0.026	0.007	0.093	0.041	0.303
3	0.024	0.030	0.015	0.008	0.110	0.031	0.220
4	0.038	0.034	0.021	0.010	0.095	0.038	0.287
5	0.032	0.046	0.020	0.004	0.095	0.049	0.340
6	0.045	0.040	0.027	0.005	0.083	0.051	0.378
7	0.023	0.025	0.013	0.003	0.113	0.031	0.216
8	0.036	0.032	0.021	0.006	0.097	0.039	0.285
9	0.067	0.038	0.025	0.014	0.071	0.060	0.460
10	0.029	0.025	0.013	0.016	0.110	0.023	0.176
11	0.072	0.041	0.019	0.008	0.068	0.066	0.490
12	0.055	0.037	0.009	0.006	0.086	0.051	0.371
13	0.070	0.051	0.025	0.008	0.061	0.071	0.534
14	0.053	0.040	0.023	0.011	0.080	0.051	0.388
15	0.056	0.041	0.022	0.019	0.079	0.051	0.392
16	0.048	0.033	0.018	0.020	0.091	0.039	0.302
17	0.053	0.065	0.046	0.000	0.060	0.081	0.572
18	0.045	0.054	0.039	0.000	0.073	0.067	0.477
19	0.058	0.063	0.041	0.000	0.058	0.080	0.581
20	0.059	0.057	0.039	0.000	0.060	0.075	0.555
21	0.040	0.015	0.016	0.018	0.107	0.025	0.190
22	0.031	0.009	0.012	0.018	0.118	0.016	0.121
23	0.020	0.010	0.016	0.021	0.124	0.011	0.084
24	0.026	0.009	0.011	0.021	0.122	0.011	0.083
25	0.036	0.030	0.012	0.014	0.102	0.031	0.234
26	0.067	0.031	0.021	0.014	0.078	0.055	0.413
27	0.032	0.035	0.011	0.012	0.104	0.033	0.243
28	0.055	0.036	0.016	0.014	0.084	0.048	0.364
29	0.060	0.047	0.019	0.018	0.076	0.057	0.428
30	0.058	0.038	0.025	0.018	0.078	0.052	0.398
31	0.049	0.040	0.020	0.018	0.085	0.046	0.349
32	0.052	0.035	0.023	0.019	0.084	0.045	0.348
33	0.084	0.064	0.046	0.000	0.034	0.097	0.743
34	0.052	0.060	0.033	0.000	0.067	0.072	0.517
35	0.110	0.080	0.061	0.000	0.000	0.129	0.998
36	0.091	0.078	0.052	0.000	0.021	0.112	0.844
37	0.070	0.016	0.024	0.020	0.086	0.053	0.383
38	0.057	0.017	0.018	0.020	0.094	0.040	0.299
39	0.032	0.012	0.015	0.027	0.116	0.014	0.107
40	0.034	0.014	0.020	0.029	0.112	0.019	0.146
41	0.060	0.062	0.031	0.000	0.061	0.076	0.557
42	0.062	0.062	0.056	0.000	0.052	0.088	0.628
43	0.047	0.060	0.028	0.000	0.074	0.068	0.479
44	0.060	0.055	0.051	0.000	0.057	0.080	0.584
45	0.034	0.009	0.019	0.019	0.113	0.020	0.152
46	0.034	0.009	0.012	0.019	0.116	0.018	0.131
47	0.031	0.015	0.017	0.017	0.112	0.020	0.150
48	0.031	0.010	0.008	0.019	0.120	0.015	0.111
49	0.067	0.035	0.023	0.012	0.073	0.058	0.443
50	0.067	0.035	0.024	0.012	0.073	0.058	0.444
51	0.067	0.035	0.025	0.011	0.072	0.059	0.449
52	0.067	0.035	0.023	0.012	0.074	0.058	0.441
53	0.067	0.035	0.023	0.012	0.074	0.058	0.440
54	0.067	0.035	0.024	0.012	0.073	0.059	0.447

4.1 Results and discussions based on TOPSIS

In this study a Box-Behnken design matrix for six factors each at three levels with 54 experiments was selected to record the experiment results. In Table 1, columns 2-7 represent the six control factors and their levels. In order to convert the multi-response optimization problem into an equivalent single response problem, the TOPSIS method was used. In Table 1, columns 9-12 represent the four responses and are illustrated as the decision matrix for the first step of the TOPSIS method. The normalized decision matrix and then the weighted normalized matrix were determined by using Eqs. (2 and 3), respectively. The criteria weights were selected as Fc = 0.4, Ft = 0.3, Fr = 0.2 and WL = 0.1. The positive ideal solution (A^{+}) and the negative ideal solution (A^{-}) could be found by Eqs. (5 and 6) as:

S^{+} = [0.1101, 0.0799, 0.0605, 0], and S^{-} = [0.0204, 0.00855, 0.0084, 0.0294]

Eqs. (7 and 8) were used to determine the separation measures. Finally, Eq. (9) was used to calculate the similarity of the ideal solutions in each scenario, ($MPCI_i$). The final results were illustrated in Table 2, last column. MPCI, i=1,2,…,54 were the surrogate responses for the proposed multi-response optimization problem. It is found that the optimal process parameter set was the 35th experiment having levels of MK2, C1, NS2, F2, CT3, and ET1 which means the 20% MK, 5% C, 70% NS, 0.5% F, CT (75 °C) and ET (25 °C). In this regard and considering the complex interaction of the investigated parameters, literatures recommended the curing temperature to be in the range between 40 °C and 85 °C for complete geopolymerization reactions [1]. Moreover, replacing FA with up to 10% C enhanced remarkably the flexural and compressive strengths of geopolymers [14]. However, the maximum compressive strength was obtained with NS/NH ratio of 2.5 [35].

4.2 Effect of process parameters on MPCI

This section presents the main effects of process parameters on MPCI of GP mortar at elevated temperature. The average responses by factor levels can be determined by using the additive property [19]. The analysis is done by averaging the data at each level of each parameter and plotting the values in graphical form. The level average responses from the data help in analyzing the trend of the performance characteristic with respect to the variation of the factor under study. The peak points of these plots correspond to the optimum condition.

Based on main effects plot as shown in **Fig. 2**, the MPCI of GP mortar was mainly affected by content of MK, C, NS, F, CT, and ET. If the MPCI is higher, the product quality will be better. From Fig. 2 the contribution of the control factors and ranks can be calculated based on delta statistics, which compare the relative magnitude of effects. The delta statistic is the highest minus the lowest average for each factor. Minitab V.16 assigns ranks based on delta values; rank 1 to the highest delta value, rank 2 to the second highest, and so on. The max–min value is equal to the range of MPCI of GP mortar due to the change in the level setting. The larger the range, the more powerful impact the control factor has on the MPCI of GP mortar.

From the analysis of Fig. 2 it was observed that the percentage contribution of the control factors affecting the MPCI of GP mortar is ET (50.1%) (Rank 1), C (12.43%) (Rank 2), CT (11.45%) (Rank 3), MK (11.2%) (Rank 4), F (10.4%) (Rank 5), and NS (4.4%) (Rank 6). Figure 2 suggests that the best levels for each control factors are, ET (Level 1), C content (Level 1), CT (Level 3), MK content (Level 2), F content (Level 2), NS content (Level 2). When analyzed main effects plot, it has been concluded that the variation of parameter ET has a great influence on MPCI of GP

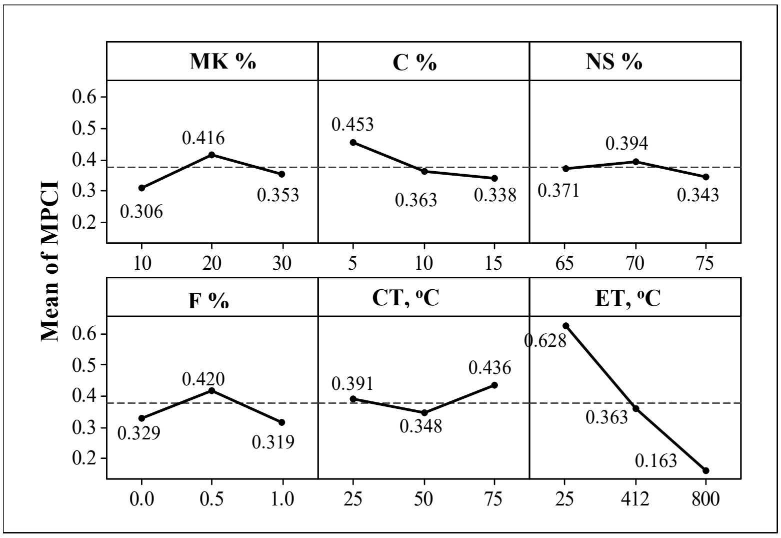

Fig. 2 - Main effects plot for MPCI of GP mortar

mortar, which decreases with parameter ET. As ET beyond 400 ^{o}C, showed a decrease in the compressive strength which increased with ET due to disintegration of the GP gel. It is revealed from the same figure that the C content has the same trend of ET. It can be interpreted in main effects plot that the MPCI increases with MK content at first, and then it decreases when MK content is varied from 20% to 30%. It can be seen from the same figure that the NS content and F content have the same trend of MK content. It is also observed that MPCI decreases with the CT at first, and then it increases when CT is varied from 50 to 75 ^{o}C.

4.3 Results and discussions based on the RSM models

4.3.1 Interaction effects of various parameters

The calculated values of MPCI are listed in Table 2 and were input into the Design Expert statistical software package. An ANOVA table (not shown) is commonly used to summarize the tests performed. Some of the model terms were found to be significant (the p-values of all significant model terms are smaller than 0.05). The insignificant model terms can be removed and may result in an improved model. The lack of fit was found to be insignificant for the responses, meaning that the lack of fit was not significant relative to the pure error. This is desirable, as a model that fits was the goal. The following equation Eq. (12) is the final empirical model of MPCI in terms of the actual factors:

$$\begin{aligned} MPCI = & -15.37 + 3.33 x MK - 2.95 x C + 42.88 x NS + 28.13 x F \\ & + 0.034 x CT - 3.99 x 10^{-4} x ET - 0.0165 MK x CT + 0.018 x C x CT \\ & + 2.167 x 10^{-3} x C x ET - 0.045 NS x CT - 1.3 x 10^{-5} x CT x ET - 5.68 x MK^2 \\ & - 29.21 x NS^2 - 2917.43 x F^2 + 5.3 x 10^{-5} x CT^2 + 2.84 x 10^{-7} x ET^2 \end{aligned} \quad (12)$$

From the developed RSM-based mathematical model, the effects of each parameter on the MPCI of GP mortar can be visualized using the interaction and response surface plots. The plots are created by considering the middle level values as the hold values of the independent variables.

Based on Eq. (12), five interactions have been found to be significant namely, MKxCT, CxCT, CxET, NSxCT, and CTxET. It is seen from the Figs. 3 and 4 that there is no interaction between the CT and C, ET and C content in affecting the MPCI of GP mortar since the responses at different levels of C content for a given level of ET and CT are almost parallel. It is revealed from Fig. 5 that there is a moderate interaction between ET and CT. From the curves at different curing temperatures in Fig. 5, it can be seen that the GP mortar possess higher MPCI at ambient temperature with higher curing temperature 75 ^{o}C until ET reaches 500 ^{o}C due to the thermolysis of –Si–O–Al–O– bond. It can be seen that the lower values of curing temperature improve the MPCI after exposure to more than 500 ^{o}C due to further geopolymerization. It is noticed from Figs. 6 and 7 that there is a slight interaction between (NS, MK), and CT in affecting the MPCI of GP mortar since the responses at different levels of CT for a given level of MK and NS are non-parallel.

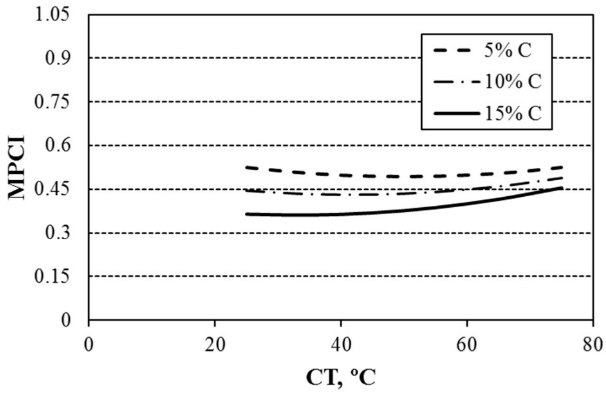

Fig. 3 - Effect of CT and C on MPCI of GP mortar

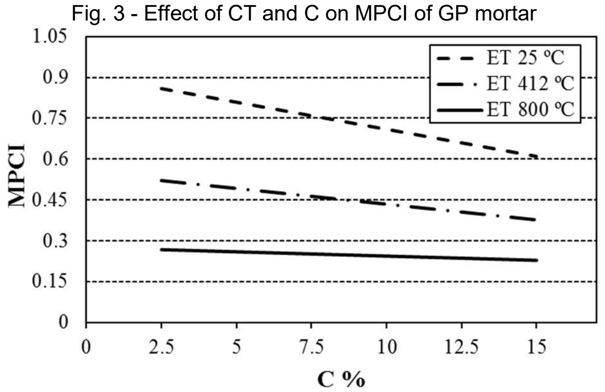

Fig. 4 - Effect of C and ET on MPCI of GP mortar

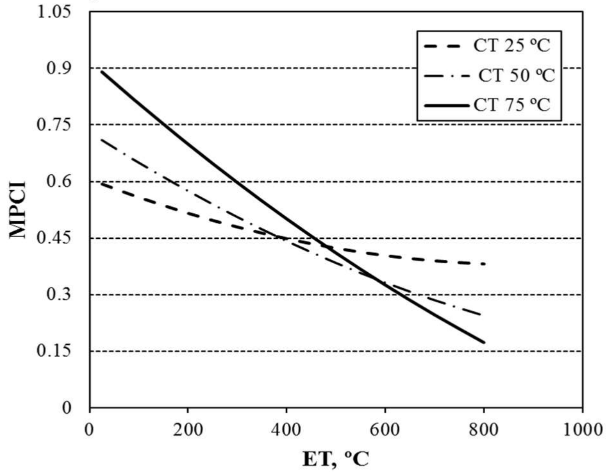

Fig. 5 - Interaction plot between ET and CT

From Figs. 3-7, it could be observed that higher MPCI of GP mortar could be obtained at increased values of MK and CT. On the other hand, a reduction in C content and ET is found to improve the MPCI of GP mortar. Fig. 8 shows a plot of MPCI distribution of GP mortar when input parameters NS and CT were varied. Low to middle level of NS and low to high range of CT favor higher value of MPCI.

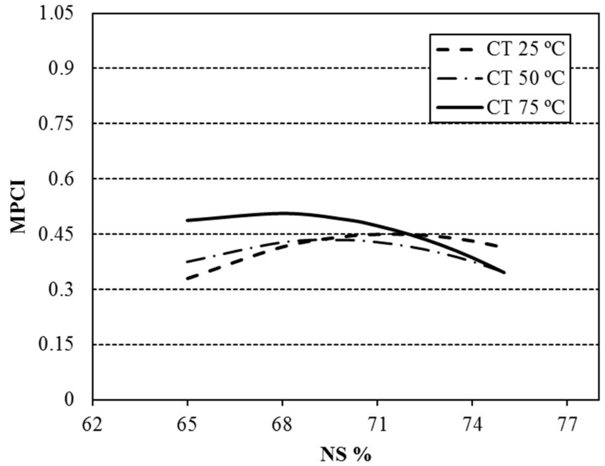

Fig. 6 - Interaction plot between NS and CT

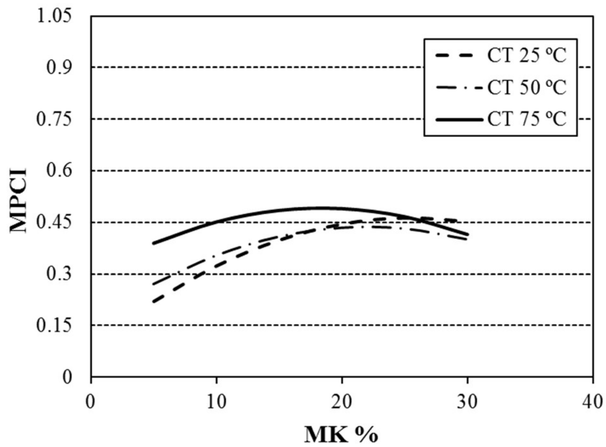

Fig. 7 - Interaction plot between MK and CT

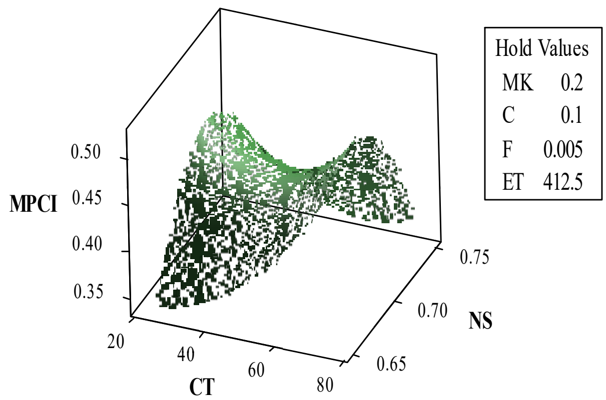

Fig. 8 - Surface plot showing the effect of two variables on MPCI

Based on the experimental **result in Table 2**, the second order RSM models for both responses, Fc and Fr were formulated as follows (Eq. (13)):

$$Fc = -1023 + 268.76xMK - 413.8xC + 2879.3xNS + 2742.57xF + 1.45xCT + 0.015xET - 1.21xMKxCT + 710xCxNS + 1.31xCxCT + 0.112xCxET - 2.27xNSxCT - 1.27xFxET - 466.57xMK^2 - 1339.45xC^2 - 2031.26xNS^2 + 0.006xCT^2 \quad (13)$$

$$Fr = -1.53 - 8.7xMK - 10.23xC + 13.63xNS + 210.4xF + 0.17xCT - 0.006xET + 74.2xMKxC - 1925xCxF - 0.32xNSxCT \quad (14)$$

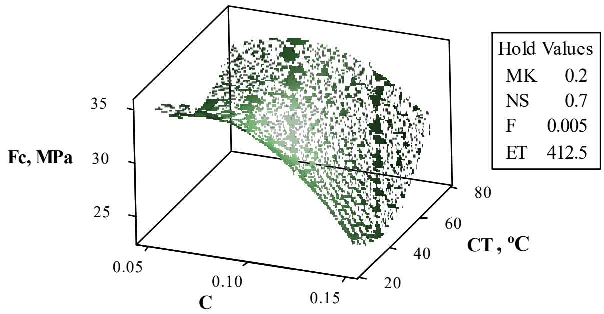

Fig. 9 - Response surface for Fc showing effect of CT and C

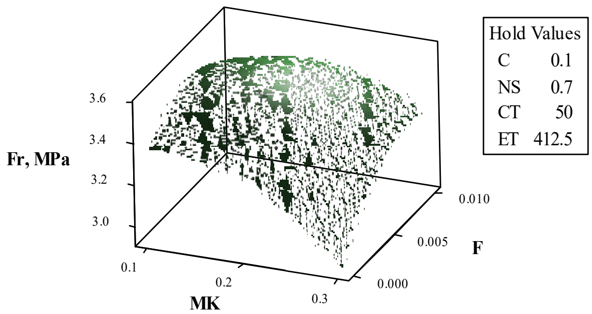

Fig. 10 - Response surface of Fr against F and MK

Figure 9 presents a three dimensional response surface plot for Fc obtained from the regression model. As can be seen from this figure, the Fc tends to increase considerably with decrease in C (because the excess of hydroxide ion concentration caused early aluminosilicate gel precipitation which affected the beneficial effect of C incorporation [14]). The Fc decreases with increase in CT. After certain level of range of 40 ºC, the Fc tends to increase. Figure 10 indicates that the increase of MK reduces the Fr of GP mortar and the increase of F increases the Fr which agrees with fiber bridging effect [9]. It should be noted that there are some conflicts in terms of recommended parameter levels obtained from the main effects plot (Fig. 2) and those obtained from the surface plots.

This can be explained by the fact that the main effect analysis is a quick and simple experimental analysis which only considers the influence of each factor individually and does not concern any interaction or squared effects. Its purpose was to quickly capture an effect of the factors to the responses. On the other hand, the RSM models included all interaction and squared effects, and in this study, it has been shown that these effects are significant.

Table 3

Summary of obtained results and sensitivity of the elevated temperatures to changes in the MPCI

Method	MK	C	NS	F	CT, °C	ET, °C	MPCI	Fc, MPa	Fr, MPa
TOPSIS (Table 2)	0.2	0.05	0.7	0.005	75	25	0.997	49.97	8
POS	0.197	0.05	0.665	0.0054	75	25	1	49.93	8.2
Optimal setting paramet ers (Eq. 12)	0.197	0.05	0.665	0.0054	75	100	0.888	46.82	7.5
						200	0.77	42.68	6.6
						300	0.657	38.5	5.74
						400	0.55	34.4	5
						500	0.45	30.25	4.15
						600	0.353	26.1	3.42
						700	0.264	22	2.73
						800	0.179	17.82	2.1

4.3.2 Results and discussions based on evolutionary PSO algorithm

TOPSIS method can only find the best specified process parameter level combination which includes the discrete setting values of process parameters, and it cannot help engineers obtain optimal process parameter when the process parameter variables are continuous. Therefore, a clear mathematical model and a systematical optimization method that can be generally used in process optimization are still required. The target of the optimization process in this study is to determine the optimal values of the process parameters that lead to the maximum value of MPCI. To formulate the optimization problem, the regression model which is proposed in Eq. (12) was taken to be the fitness function of the optimization solution. The maximization of the fitness function value of Eq. (12) was subjected to the boundaries (limitations) of the process parameters. The range of each experimental parameter in Table 1 was selected to present the limitations of the optimization solution and is given as follows:

$0.1 \le MK \le 0.3$, $0.5 \le C \le 0.15$, $0.65 \le NS \le 0.75$, $0.005 \le F \le 0.01$, $25 \le CT \le 75$, and $25 \le ET \le 800$

In order to optimize the present problem using PSO, the following parameters have been selected to obtain optimal solutions with less computational effort. No. of interactions = 1000, $c1$=2, $c2$=2, and w=0.5. The PSO code was developed using MATLAB. Two MATLAB script files (*. m) are needed to fully write the codes. In the first file, the objective function Eq. (12) (fitness function) is defined, whereas in the second file, the main PSO program is developed.

The set values of optimal process parameters that lead to the maximum MPCI value are 19.7% for MK, 5% for C, 66.5% for NS, 0.54% for F, 75 °C for CT, and 25 °C for ET. By transferring the optimal process values into the Fc and Fr equations, it was obtained that Fc = 49.93 MPa and Fr = 8.2 MPa. Optimum result was further validated through follow up experiment. The optimal setting parameters at different values of the elevated temperature can be used to illustrate the sensitivity of the elevated temperatures to the changes in the MPCI of GP mortar. The obtained results and sensitivity of the elevated temperature to changes in the MPCI of GP mortar are listed in Table 3. It can be seen that the percentage deviation of the simulated result from experimental reading indicates the real-world applicability of the results with this specific search space.

5. Conclusions

In this work, a process modeling and optimization for a desired MPCI of GP mortar at elevated temperature has been performed by using experimental design, TOPSIS, statistically based modeling and particle swarm optimization methods PSO. The application of the proposed method was proven to be useful for obtaining the optimal process parameters for a desired MPCI of GP mortar at elevated temperature. The following is a summary of other important findings:

1. The approach and the methodologies employed in this work can be utilized in solving the mixture proportions of the optimization problem.
2. The GP mortar consisting of 19.7% MK, 5% C, 66.5% NS, 0.54% F, CT (75 °C), and ET (25 °C) provides optimum MPCI at ambient temperature, and it is suited for elevated temperature applications.
3. The purpose of developing the mathematical model is to facilitate the optimization of GP mortar process at elevated temperature. Therefore, a PSO algorithm-based procedure has been used to predict the best process parameters values at any desired elevated temperature.
4. The percentage contribution of the control factors affecting the MPCI of GP mortar is ET (50.1%), C (12.43%), CT (11.45%), MK (11.2%), F (10.4%), and NS (4.4%).
5. The GP mortar possess higher MPCI with higher curing temperature (CT) 75 °C until ET

reaches 500 °C. However, the lower values of curing temperature (CT 25 °C) improve the MPCI after exposure to more than ET 500 °C.

6. The MPCI increases with MK content up to 20%, and then it decreases when MK content is varied from 20% to 30%.

Conflict of interest
The authors declare that they have no conflict of interest.

REFERENCES

[1] B. Singh, G. Ishwarya, M. Gupta, S.K. Bhattacharyya, Geopolymer concrete: A review of some recent developments, Constr. Build. Mater., 2015, 85, 78-90.
[2] D.L.Y. Kong, J.G. Sanjayan, Effect of elevated temperatures on geopolymer paste, mortar and concrete, Cem. Concr. Rese.,2010, 40, 334-339.
[3] S. Mane, H.S. Jadhav, Investigation of geopolymer mortar and concrete under high temperature, Inter. J. Emer. Tech. Adva. Eng. IJETAE, 2012, 2(21), 384-390.
[4] F.U.A. Shaikh, V. Vimonsatit, Compressive strength of fly ash-based geopolymer concrete at elevated temperatures, Fire and Mater., 2014, 39, 174-188.
[5] D.L.Y. Kong, J.G. Sanjayan, Damage behavior of geopolymer composites exposed to elevated temperatures, Ceme. Concr. Compo., 2008, 30, 986-991.
[6] P.K. Sarker, T. de Meillon, Geopolymer concrete after exposure to high temperature heat, recent developments in structural engineering. In: Zingoni A, editor, Mechanics and Computation, Rotterdam, The Netherlands: Millpress, 2007, 1566-1571.
[7] P.K. Sarker, S. Kelly, Z. Yao, Effect of fire exposure on cracking, spalling and residual strength of fly ash geopolymer concrete, Mater. Desi., 2014, 63, 584-592.
[8] H.Y. Zhang, V. Kodur, S.L. Qi, L. Cao, B. Wu, Development of metakaolin-fly ash based geopolymers for fire resistance applications, Constr. Build Mater., 2014, 55, 38-45.
[9] Z. Yunsheng, S. Wei, Z. Li, Z. Xiangming, Geopolymer extruded composites with incorporated fly ash and polyvinyl alcohol short fiber, ACI Mater. J., 2009, 106(1), 3-10.
[10] L. Vickers, A. Riessen, W.D.A. Rickard, Fire-resistant geopolymers role of fibres and fillers to enhance thermal properties, Springer Briefs in Materials, Springer Singapore Heidelberg New York Dordrecht London, 2015, 135.
[11] G.F. Peng, W.W. Yang, J. Zhao, Y.F. Liu, S.H. Bian, L.H. Zhao, Explosive spalling and residual mechanical properties of fiber-toughened high-performance concrete subjected to high temperatures, Cem. Concr. Rese., 2006, 36, 723-727.
[12] H. Zhang, V. Kodur, L. Cao, S. Qi, Fiber reinforced geopolymers for fire resistance applications, Proc. Eng., 2014, 71, 153-158.
[13] P. Nath, P.K. Sarker, Use of OPC to improve setting and early strength properties of low calcium fly ash geopolymer concrete cured at room temperature, Cem. Conc. Comp., 2015, 55, 205-214.
[14] T. Phoo-ngernkham, V. Sata, S. Hanjitsuwan, C. Ridtirud, S. Hatanaka, P. Chindaprasirt, Compressive strength, bending and fracture characteristics of high calcium fly ash geopolymer mortar containing Portland cement cured at ambient temperature, Arab. J. Scie. Eng., 2016, 41, 1263-1271.
[15] F. Bektas, B. Aldemir, Analyzing mix parameters in ASR concrete using response surface methodology, Constr. Build. Mater., 2014, 66, 299-305.
[16] M.M. Rahman, M.A.R. Khan, M.M. Noor, K. Kadirgama, R.A. Bakar, Optimization of machining parameters on surface roughness in EDM OF TI-6AL-4V using response surface method, Adva. Mater. Rese., 2011, 213, 402-408.
[17] M.F. Ghazy, Effect of using mortar interface and overlays on masonry behavior by using Taguchi method, ACI Mater. J., 2012, 109(5), 509-516.
[18] M. Olivia, H. Nikraz, Properties of fly ash geopolymer concrete designed by Taguchi method, Mater. Desi., 2012, 36, 191-198.
[19] M.A.A. Abd Elaty, M.F. Ghazy, M.F. Abd El Hameed, Optimization of geopolymer concrete by principal component analysis, ACI Mater. J., 2017, 114(2), 253-264.
[20] M.F. Ghazy, M.F. Abd El Hameed, Optimization of lightweight concrete process by Gray-Taguchi method, ACI Mater J., 2015, 112(3), 365-374
[21] B. Simsek, Y.T. Iç, E.H. Simsek, A TOPSIS-based Taguchi optimization to determine optimal mixture proportions of the high strength self-compacting concrete, Chem. Intell. Labo. Syst., 2013, 125, 18-32.
[22] ASTM C618-19, Standard specification for coal fly ash and raw or calcined natural pozzolan for use in concrete, American Society for Testing and Materials, West Conshohocken, PA, USA: ASTM International, 2019.
[23] EN 197-1, Cement composition, specifications and conformity criteria for common cements, European Committee for Standardization, 2018.
[24] ASTM C33, Standard specification for concrete aggregates, American Society for Testing and Materials, West Conshohocken, PA, USA: ASTM International, 2018.
[25] ASTM C1437, Standard test method for flow of hydraulic cement mortar, American Society for Testing and Materials, West Conshohocken, PA, USA, ASTM International, 2020.
[26] EN 196-1:2016, Methods of testing cement determination of strength, European Committee for Standardization, 2021.
[27] NBR 7222:2011, Concrete and mortar - Determination of the tension strength by diametrical compression of cylindrical test specimens, Brazilian Standards, 2013.
[28] M.F. Abd El Hameed, M.F. Ghazy, M.A.A. Abd Elaty, Optimisation of adhesive anchors in concrete by desirability function, Maga. Concr. Rese., 2015, 67(20), 1101-1111.
[29] M.A.A. Aldahdooh, N.M. Bunnori, M.A.M. Johari, Evaluation of ultra-high performance-fiber reinforced concrete binder content using the response surface method, Mater. Desi., 2013, 52, 957-965.
[30] R.H. Myers, D.C. Montgomery, Response surface methodology: process and product optimization using designed experiments, 3rd ed Handbook, Hoboken, Wiley 677, 2002.
[31] C.L. Hwang, K. Yoon, Multiple attribute decision making methods and applications, Springer Verlag Berlin 186, 1981.
[32] V.S. Gadakh, Parametric optimization of wire electrical discharge machining using TOPSIS method, Adva. Prod. Eng. Manag., 2012, 7(3), 157-164.
[33] J. Kennedy, R.C. Eberhart, Particle swarm optimization, Proceedings of IEEE International Conference on Neural Networks, IEEE Service Center, Piscataway, 1995, 4, 1942-1948.
[34] A. Lazinica, Particle Swarm Optimization, Publisher: In-Tech, 2009.
[35] Z. Yahya, M.M. Abdullah, K. Hussin, K.N. Ismail, R. Abd-Razak, A.V. Sandu, Effect of solids-to-liquids, Na_2SiO_3-to-NaOH and curing temperature on the palm oil boiler ash (Si + Ca) geopolymerisation system, Mater., 2015, 8, 2227-2242.

.

****